

# Domain morphology in polyurethanes

K. W. Chau and P. H. Geil

Polymer Group, Department of Metallurgy & Mining Engineering, University of Illinois, Urbana, Illinois 61801, USA

(Received 5 December 1983; revised 30 July 1984)

The domain morphology of a polyurethane has been visualized by dark field electron microscopy. Ageing of both as-cast and drawn films results in an increase in size and perfection of the soft segment domains over an extended period of time. Annealing taut drawn films above the melting point of the soft segment results in a complete rearrangement of the morphology. The dark field studies are supplemented by electron microscopic observations of replicas and stained samples and correlated with corresponding changes in physical properties.

(Keywords: domain morphology; polyurethanes; dark field electron microscopy; films)

## INTRODUCTION

Polyurethanes are chosen for many broad and varied applications, primarily because they can be prepared with relative ease, at low cost, from a wide variety of raw materials. Depending upon the specific end use, the chemist can design a material which is either primarily elastic or rigid in nature by merely varying the chemical constituents of the polymer. Although polyurethane chemistry has been extensively characterized over the past three decades, only recently has there been much emphasis on characterizing the morphological features which are responsible for the physical and mechanical properties. One must consider here such factors as composition, hydrogen bonding, phase separation, and orientation for attainment of the desired properties.

Most commercial polyurethanes are prepared by a random, linear condensation of stoichiometric amounts of an aromatic or aliphatic diisocyanate, a low molecular weight glycol or diamine, and a polyester or polyether macroglycol. In elastomeric polyurethanes, the macroglycol of the polymer chain is above its glass transition temperature ( $T_g$ , typically between  $-20^\circ\text{C}$  and  $-80^\circ\text{C}$ ) at service temperatures and forms the soft segment. The diisocyanate group coupled with a low molecular weight glycol or diamine chain extender has a  $T_g$  (typically between  $90^\circ\text{C}$  and  $130^\circ\text{C}$ ) above service temperatures and forms the hard segment. Each polyurethane chain consists of alternating hard and soft segments which are joined end to end through covalent (urethane or urethane-urea) bonds. Polyurethanes are thus classified as multiblock copolymers.

The physical properties of thermoplastic, elastomeric polyurethanes have been characterized by a number of workers. Schollenberger and co-workers<sup>1</sup> first proposed the concept of hydrogen bonding or 'virtual-crosslinking' to explain the origin of the high tensile strength of polyurethanes. Cooper and Tobolsky<sup>2</sup> compared the viscoelastic response of selected polyurethanes with that of other polymers. The polyurethanes exhibited an anomalously high modulus well above their soft-segment  $T_g$ , unaccounted for by either chemical crosslinking or crystallinity. The similarity between their viscoelastic re-

sponse and that of known block copolymers along with the detection of two  $T_g$ 's led them to conclude that two phases existed in polyurethanes. It is usually suggested<sup>3,4</sup> that, as a result of phase separation and, in some cases, hydrogen bonding, the two types of segments tend to aggregate individually to form domains which act as tie points or virtual crosslinks between linear polyurethane chains such that the materials possess the physical characteristics and mechanical behaviour at room temperature of a covalently crosslinked network.

The study of polyurethane block copolymers by wide-angle X-ray diffraction (WAXD) and small-angle X-ray scattering (SAXS) techniques has given valuable information about their internal structure. Shimanskii *et al.*<sup>5</sup> detected some ordering in the hard-segment domains in certain samples. Clough and Schneider<sup>6</sup> showed that strain-induced crystallization of the soft segments occurred at extensions of 180% and 150% for elastomers based on poly(oxytetramethylene) glycol or poly(tetramethylene adipate) with diphenylmethane-4,4'-diisocyanate and 1,4-butanediol. SAXS studies carried out by Clough *et al.*<sup>7</sup> showed that structural ordering in domains occurred in these and other similar materials. The domain structure was usually noncrystalline although crystallization could occur in samples which contained sufficiently long hard or soft segments.

Clough and co-workers<sup>6,7</sup> and also Schollenberger<sup>8</sup> used differential scanning calorimetry to determine the transition temperature ranges in various domains due to melting, hydrogen bond dissociation and the glass transitions. They showed that the extent of phase segregation was proportional to the urethane content of the polymer.

Of more direct concern here is the WAXD and differential thermal analysis study carried out by Bonart and co-workers<sup>9,10</sup>, on several similar polyurethane systems, all of which had strong potential for hydrogen bonding. Although the as-cast films showed only amorphous X-ray diffraction patterns, thermal treatment and tensile deformation induced crystallization as indicated by X-ray diffraction. In these treated systems, it was possible to distinguish the diffraction produced by the strain-crystallized polyester or polyether soft segments

from that produced by the oriented hard-segment domains. Using a paracrystalline model for the packing of the seemingly liquid-crystal-like hard segment domains, they used optical diffraction techniques to justify their model in which the ordering in the hard segment domains was due to a system of hydrogen bonds.

More recently, Bonart and co-workers<sup>11-13</sup> used SAXS techniques to quantitatively compare the extent of phase separation in polyether *versus* polyester urethanes and in polyurethanes differing only in the length of the aliphatic diol chain extender. In addition they characterized the similarities and differences in hard-segment structure in polyurethanes extended with diamines *versus* diols. They demonstrated the possibility of calculating a number of parameters, such as phase boundary diffuseness, width of diffuse transition zones, specific internal surface area and fraction of sharp boundaries as well as domain size. Unfortunately the results were not as conclusive as would be desired.

Although the above work was done on samples in which hydrogen bonding was presumed to be the basis of cohesion of the hard-segment domains, current concepts are shifting towards viewing simple phase segregation as the origin of reinforcement in elastomeric polyurethanes. Harrell<sup>14</sup> demonstrated that piperazine-based polyurethanes, which are incapable of hydrogen bonding, still produced phase segregation and desirable tensile properties.

Depending on thermal and physical treatment a number of types of domain morphology are possible. For instance Wilkes and Yusek<sup>15</sup> suggested the following types of domains in a typical hydrogen-bonding oriented polyurethane: (1) Crystalline soft segment domains whose crystallinity may either be the result of strain-induced crystallization or, depending on prior heat treatment, molecular weight and stereoregularity; the domain may exhibit crystallinity in the unstressed state; (2) oriented, noncrystalline soft segment domains; (3) amorphous 'solutions' of hard and soft segments; (4) crystalline hard-segment domains; and (5) oriented, noncrystalline hard-segment domains. The same types of domains might be expected in unoriented systems except that the domains will be randomly oriented. The five types of domains contain the structural features necessary to attain polymer properties ranging from elastomeric to plastic. Other models, however, have also been suggested; an example is one in which the hard segments form an interlocking network cocontinuous with regions rich in soft segments<sup>16</sup>. Results from X-ray diffraction studies<sup>10,15</sup> allowed one to conclude that the spacing between centres of neighbouring like domains in polyurethanes typically measures from 200 Å to 300 Å, depending on segment lengths.

Findings from previous research concerning the relationship between physical, thermal and mechanical properties of polyurethanes and their chemical compositions are summarized in review articles by Van Bogart *et al.*<sup>17</sup> and by Abouzahr and Wilkes<sup>18</sup>. However, there are relatively few published reports in the literature concerning the study of domain morphology with transmission electron microscopy. Schneider *et al.*<sup>19</sup> obtained transmission electron micrographs of coarse, poorly formed spherulites believed to be composed of hard-segment rich fibrils measuring 200 Å to 600 Å. Chang *et al.*<sup>20</sup> observed hard-segment rich globules and spherulites

of the order of tens of microns in size as well as hard-segment rich fibrils of the order of 100 Å wide in reaction injection moulded polyurethanes. Recently, Briber and Thomas<sup>21</sup> presented evidence of the formation of two different types of spherulites by diphenylmethane-4,4'-diisocyanate/1,4-butanediol hard segments. They were able to obtain a dark-field micrograph showing individual diffracting lamellae formed by the hard segments.

A significant problem in the studies of polyurethanes is obtaining sufficient contrast in electron micrographs to visualize the domains. Since even highly phase segregated polymeric systems will possess regions of similar electron density, mass thickness contrast will be intrinsically low. The technique of heavy atom staining to increase mass thickness contrast depends on finding a selective stain. Iodine staining was used in one study<sup>22</sup> but it was complicated by the unknown solubility and chemical specificity of iodine in the different phases. The domain morphology suggested by the micrographs was not verified by other techniques. Other workers have attempted staining with phosphotungstic acid<sup>23</sup> and osmium tetroxide<sup>24</sup> but have had only limited success.

Phase contrast imaging has long been known as a way of enhancing image contrast<sup>25</sup>. Its application to biological specimens has been investigated in detail<sup>26</sup>. A number of researchers<sup>27,28</sup>, by making use of this technique, claimed to be successful in directly visualizing polyurethane domains.

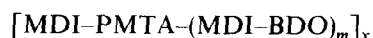
However, the complex problem of image formation due to phase differences introduced by the microscope system as well as the object make interpretation of the images difficult, particularly for domain structures at the 100 Å scale and below. Recent studies<sup>29,30</sup> of the phase contrast technique seriously question its reliability in the observation of polyurethane domains and cast doubts upon the validity of previous micrographs of polyurethanes with this technique.

The aim of the present research was to examine suitable techniques and apply them to characterize the morphological features responsible for the physical properties of polyurethanes. In particular, emphasis was placed on studying the conditions for domain formation (such as effects of different solvents, casting conditions, annealing and tensile deformation) and techniques for direct electron microscope observations of the domains. In addition, other techniques such as wide- and small-angle X-ray diffraction and differential scanning calorimetry (d.s.c.) were applied to characterize the crystallinity, degree of phase separation, orientation and domain structure.

## EXPERIMENTAL

### Materials

Two commercial polyurethanes produced by the B. F. Goodrich Company were studied. Designated Estane 5712 and Estane 5707, they were prepared by the copolymerization of poly(tetramethylene adipate) glycol (PTMA) with 1,4-butanediol (BDO) and diphenylmethane-4,4'-diisocyanate (MDI). The polyurethanes used were supplied in the form of pellets and have the chemical structure



The compositions of the two samples are shown in Table 1.

**Table 1** Sample compositions

Sample	Number average molecular weight of PTMA ( $M_n$ )	$m$
Estane 5712	3100	0.3
Estane 5707	1600	2.0

Accordingly, the hard segment in Estane 5712 is either MDI-BDO-MDI (extended segment length = 36 Å) or an MDI alone (extended segment length = 14 Å). The average hard segment in Estane 5707 is MDI-BDO-MDI-BDO-MDI which has an extended segment length of 58 Å. The calculated extended lengths of the soft (PTMA) and hard (MDI-BDO) segments in the two polyurethanes are shown in *Table 2*. The various segment lengths are based on bond angles and lengths given by Morrison and Boyd<sup>31</sup>. Other values for the MDI-BDO segment lengths have been given (19 Å<sup>32</sup> and 20.3 Å<sup>10</sup>) but will not affect our conclusions.

#### Sample preparation

**Solution casting of Estane 5712.** Solution-cast films of Estane 5712 were prepared from a solution in 1,2-dichloroethane, *N,N*-dimethyl formamide (DMF), or tetrahydrofuran (THF). Thin films ( $\approx 1000$  Å thick) for transmission electron microscopy were prepared by spreading a few drops of a 1% (by weight) solution on water or alternatively on a carbon coated glass slide. The solvent was allowed to evaporate in air at room temperature. The films cast on water were directly picked up on 200 mesh copper electron microscope grids. The films cast on carbon coated glass slides were cut into 1 mm squares, floated off on water and picked up on electron microscope grids. The carbon coating acted as a release agent for the tacky polyurethane which would otherwise adhere firmly to the clean glass surface.

Uniaxially oriented thin films were prepared by casting a few drops of 1% solution in 1,2-dichloroethane on water and stretching the resulting films with a draftsman's divider with bent ends before placing them on electron microscope grids. The tackiness of Estane 5712 kept the drawn films from retracting once they adhered to the grids. DMF and THF solutions were found to be unsuitable for this purpose because those two solvents are highly soluble in water, leaving broken polyurethane films.

Thick films ( $\approx 0.1$  mm thick) for X-ray diffraction and d.s.c. studies were obtained from a more concentrated solution prepared by dissolving 10 g of Estane per 100 ml of solvent and refluxing the mixture at the boiling point of the pure solvent for 24 h. The solution was cast on a block of Teflon\* kept level by floating it on mercury to ensure uniform film thickness. The solvent was allowed to evaporate in air at room temperature.

**Solution casting of Estane 5707.** Only DMF and THF were used as solvents for Estane 5707 since it is insoluble in 1,2-dichloroethane. Two casting methods were studied:

(i) Room-temperature casting was carried out with solutions in the two different solvents in the same manner as described for Estane 5712. Clean glass slides without carbon coating could be used as Estane 5707 is less tacky.

(ii) Elevated-temperature casting was carried out following Briber and Thomas<sup>21</sup> by spreading some DMF solution on a carbon coated glass slide. The solvent was allowed to evaporate in a covered glass petri dish which contained about 7–10 ml of pure DMF at the bottom. The petri dish was kept in an oven at 135°C. Casting by this method resulted in slow evaporation of solvent at an elevated temperature. About 10–12 h were required for complete solvent evaporation. Only DMF solution was suitable for this method since THF has a boiling point substantially below 135°C. Thin films ( $\approx 1000$  Å thick) prepared by this method were cut into 1 mm squares with a razor blade, floated off on water and picked up on electron microscope grids. Thick films ( $\approx 0.1$  mm thick) prepared by this method could be peeled off from the glass slide with a pair of tweezers.

**Selective staining.** The polyester phase was stained with osmium tetroxide ( $OsO_4$ ) by suitably modifying a method reported by Wegner *et al.*<sup>33</sup> as discussed below. Estane 5712 thin films to be stained were prepared by casting on water a few drops of a 1% solution in a solvent composed of a mixture of 1,2-dichloroethane and allyl amine in a 4:1 volume ratio. Estane 5707 thin films were prepared by casting on clean glass slides a few drops of 1% solution in a solvent composed of DMF and allyl amine in a 4:1 ratio. The solvent was allowed to evaporate in air. The thin films were cut, floated off on water, picked up on electron microscope grids, put in a  $10^{-5}$  torr vacuum for 6 h and kept for selected periods of time at room temperature above a dish of a 1%  $OsO_4$  aqueous solution inside a covered glass jar.

The staining technique developed by Wegner and co-workers makes use of the supposed preferential absorption of allyl amine by the polyester crystalline boundaries and the  $OsO_4$  chemical attacks on the C=C double bond present in the allyl group. In their method, the copolymer thin film is dipped in allyl amine in order that the allyl amine be absorbed and the sample is subsequently stained by exposure to  $OsO_4$  vapour. The technique was modified for our Estane polyurethanes because they readily dissolve in allyl amine.

**Compression moulding.** Compression moulded films were prepared by placing polyurethane pellets in a mould consisting of a 6 cm  $\times$  9 cm window cut out of a piece of 1 mm thick brass plate sandwiched between two pieces of 1 mm thick Teflon sheets. They were melted at 190°C for 5 min in a Carver Press equipped with heating plates, pressed for another 5 min at a pressure of 2000 psi, and quenched into 20°C water. Teflon sheets were used instead of metal foils because, when cooled from the melt, polyurethanes stubbornly adhere to metal surfaces, rendering the subsequent removal of metal foils difficult.

**Table 2** Calculated extended lengths of hard and soft segments in the polyurethane samples

Sample	Average extended soft segment length	Extended hard segment length
Estane 5712	227 Å	14 Å or 36 Å
Estane 5707	117 Å	58 Å

\* Trademark of E. I. duPont de Nemours &amp; Co., Inc.

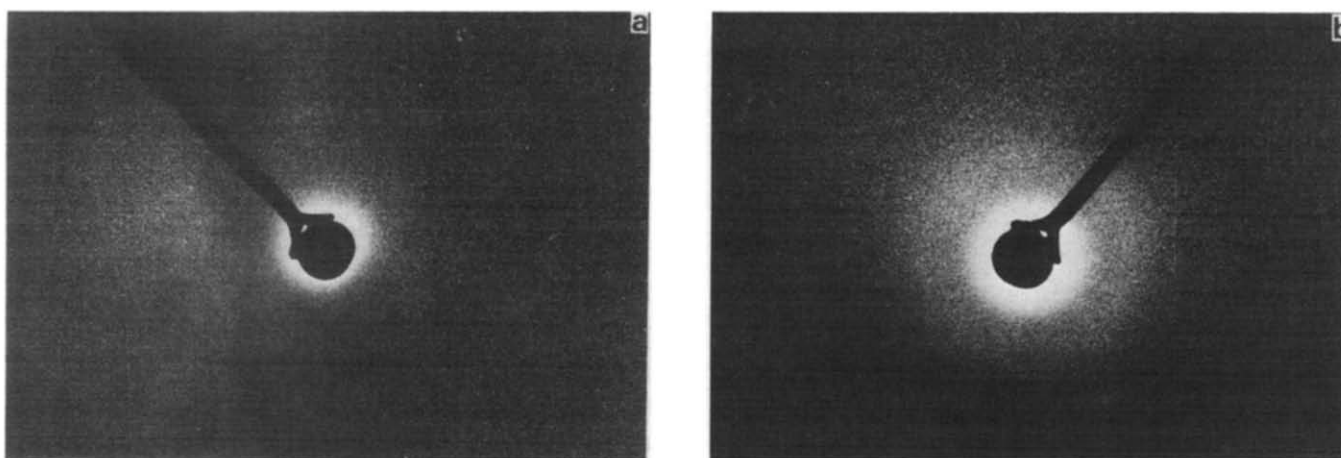


**Figure 1** SAXS pattern of 1,2-dichloroethane solution-cast Estane 5712 thick films. (a) aged for two days at room temperature; (b) aged for one month at room temperature

#### Wide-angle X-ray diffraction

A flat plate camera with a sample to film distance of 5 cm was used for the purpose. WAXD patterns of stacked solution-cast thick films (with a total thickness of 1 mm) as well as compression moulded films were taken using  $\text{CuK}\alpha$  radiation.

#### Small-angle X-ray scattering

SAXS patterns were recorded with a Rigaku-Denki SAXS camera. Both compression moulded films and stacked solution-cast thick films (of a net thickness 1 mm) were studied.

#### Differential scanning calorimetry

D.s.c. studies were made using a DuPont 1090 thermal analyser equipped with a 910 differential scanning calorimeter and a 1091 disc memory. The heating rate was  $20^\circ\text{C min}^{-1}$ . Sample size was 3–5 mg. Data analysis was carried out with computer software provided by DuPont Instruments Inc.

#### Transmission electron microscopy

Carbon/platinum free surface replicas of thick films were prepared using a one-stage method with polyacrylic acid. Thin films, whose surface morphology was to be studied, were shadowed with C/Pt at a  $30^\circ$  angle just prior to examination. Samples to be examined with diffraction contrast imaging techniques were lightly coated with carbon at a  $90^\circ$  angle just prior to examination. This carbon coating improved the electrical conductivity of the polyurethane films and prevented the accumulation of electric charge. The microscope used was a JEOL JEM 100C which was operated at 100 kV.

#### Tensile testing

An MTS T5002 tensile tester was used for the stress-strain studies. Specimens used were of dumb-bell shape with a gauge length of 5 cm, a width of 1.2 cm, a thickness of 0.1 cm, and a crosshead speed of  $3\text{ cm min}^{-1}$ . Stress-strain curves were plotted directly by the MTS machine.

## RESULTS

### Estane 5712

The SAXS patterns of the same stack of 1,2-dichloroethane solution-cast thick films taken after different

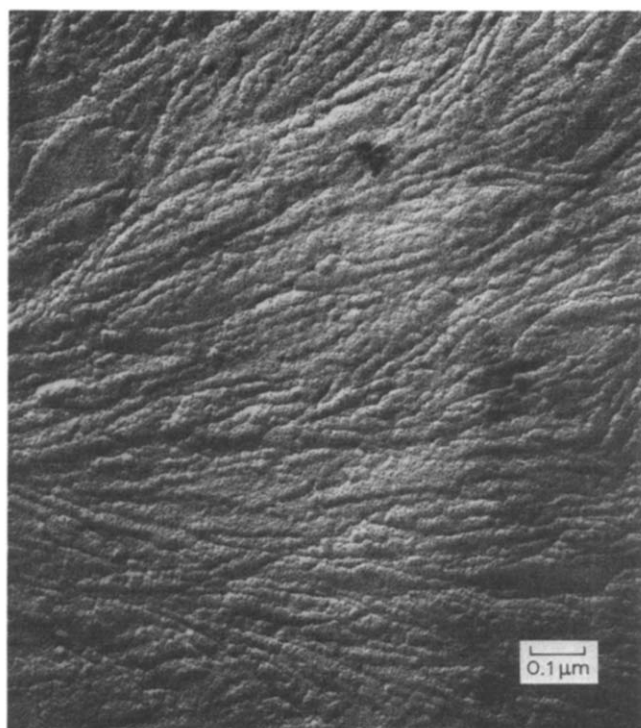


**Figure 2** Typical free surface replica of 1,2-dichloroethane solution-cast Estane 5712 thick film (aged for three months at room temperature), showing a portion of a spherulite

periods of room-temperature ageing are shown in *Figure 1*. The scattering pattern of the freshly cast films (*Figure 1a*) only shows some diffuse scattering. However, a scattering intensity maximum corresponding to a long period spacing of  $\approx 200\text{ \AA}$  appears on ageing (*Figure 1b*). Free surface replicas of such aged solution-cast thick films reveal a spherulitic morphology. The spherulites appear to be composed of radially oriented fibrils (*Figure 2*). The spacing between neighbouring fibrils is  $180\text{ \AA}$ – $250\text{ \AA}$ . A similar surface morphology and ageing effect on the SAXS period was found in thick films prepared by heat moulding or by casting from a DMF or THF solution.

D.s.c. scans of the 1,2-dichloroethane solution-cast thick films (*Figure 3*) show a major crystalline melting transition in the  $40^\circ\text{C}$ – $60^\circ\text{C}$  range. It is noted that the heat of transition increases from  $28.2\text{ J g}^{-1}$  to  $34.2\text{ J g}^{-1}$

on ageing at room temperature for one year. The crystalline melting peak increases from 45.3°C to 48.6°C. The  $T_g$  of the soft segment, however, remains constant at approximately -36°C. Films cast from DMF and THF solutions show similar behaviour. D.s.c. scans of compression moulded films differ from solution cast films only in that the  $T_g$  of the soft segments decreases from -33.7°C to -37.9°C after being aged one year.

Spherulites also form in solution-cast thin films (Figure 4). Electron diffraction patterns of such thin films reveal reflections consistent with those of the  $\beta$  polymorph of PTMA crystals previously reported by Minke and Blackwell<sup>34</sup>. Although the  $\beta$  form PTMA crystals in their sample transformed into the more stable  $\alpha$  form after one week of room temperature ageing, no phase transformation has been detected in Estane 5712 after an ageing

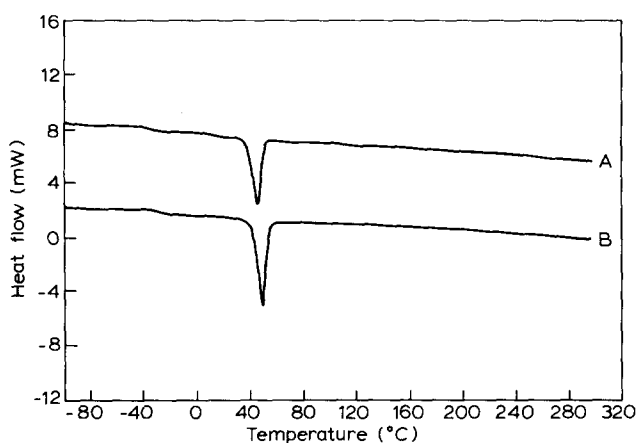


Figure 3 D.s.c. scans of 1,2-dichloroethane solution-cast Estane 5712 thick films. Curve A: aged for one day at room temperature; curve B: aged for one year at room temperature

time of one year. Dark-field diffraction contrast electron micrographs (imaged with the 3.74 Å (020) and 4.18 Å (110) reflections, shown in Figure 5, reveal that such spherulites are composed of radial aggregates of commonly oriented soft-segment domains. A typical OsO<sub>4</sub> stained area is shown in the micrograph of Figure 6. It can be seen that not only the crystal boundaries but the PTMA polyester crystalline domains themselves were stained and appear dark throughout. Their size and shape agree well with that from dark-field microscopy in Figure 5.

Tensile deformation breaks down the spherulite (Figure 7). In the dark-field micrographs of the drawn samples (Figure 8), the resulting crystalline domains are seen as lamellae of thickness from  $\approx 200$  Å to  $\approx 300$  Å and width from  $\approx 600$  Å up to 2000 Å. For a draw ratio of 4 to 6, they orient with their width perpendicular to the draw direction (Figure 8). The draw direction in the micrographs was determined by examining the drawn films with an optical microscope.

The micrographs in Figure 5 and 8 show the effect of room temperature ageing. The domains become larger and the crystalline perfection within improves (the diffraction pattern becomes sharper and more intense, and the domains become more stable to exposure in the electron beam). The average size of the domains seems to reach an asymptotic limit after one month (Figures 8c and d). The surface morphology of as-cast films is also affected (Figure 4a and b), implying movement on the surface as well. If an oriented sample is annealed taut at a temperature which is above the melting point of PTMA crystals although substantially below the melting point of MDI-BDO crystals, a total rearrangement occurs and the previously induced orientation is destroyed (Figure 9).

The mechanical properties of Estane 5712 following heat moulding or solution casting are highly time de-

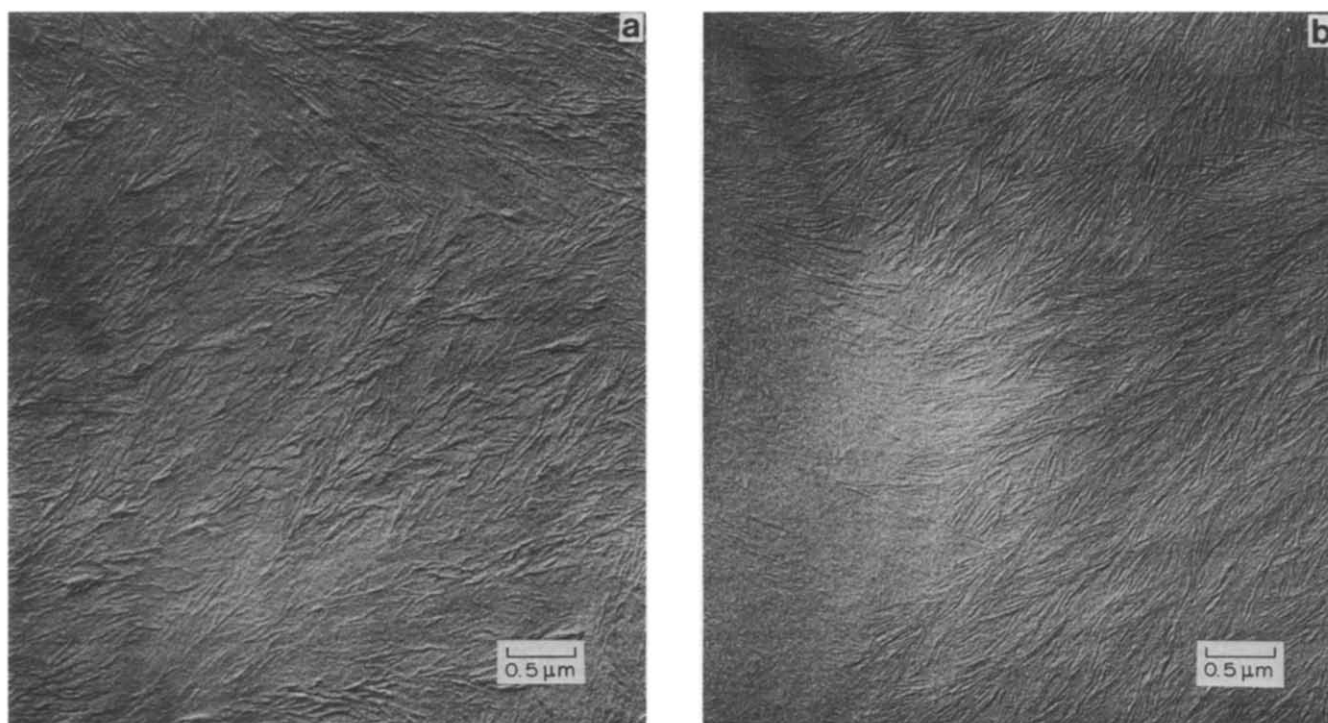
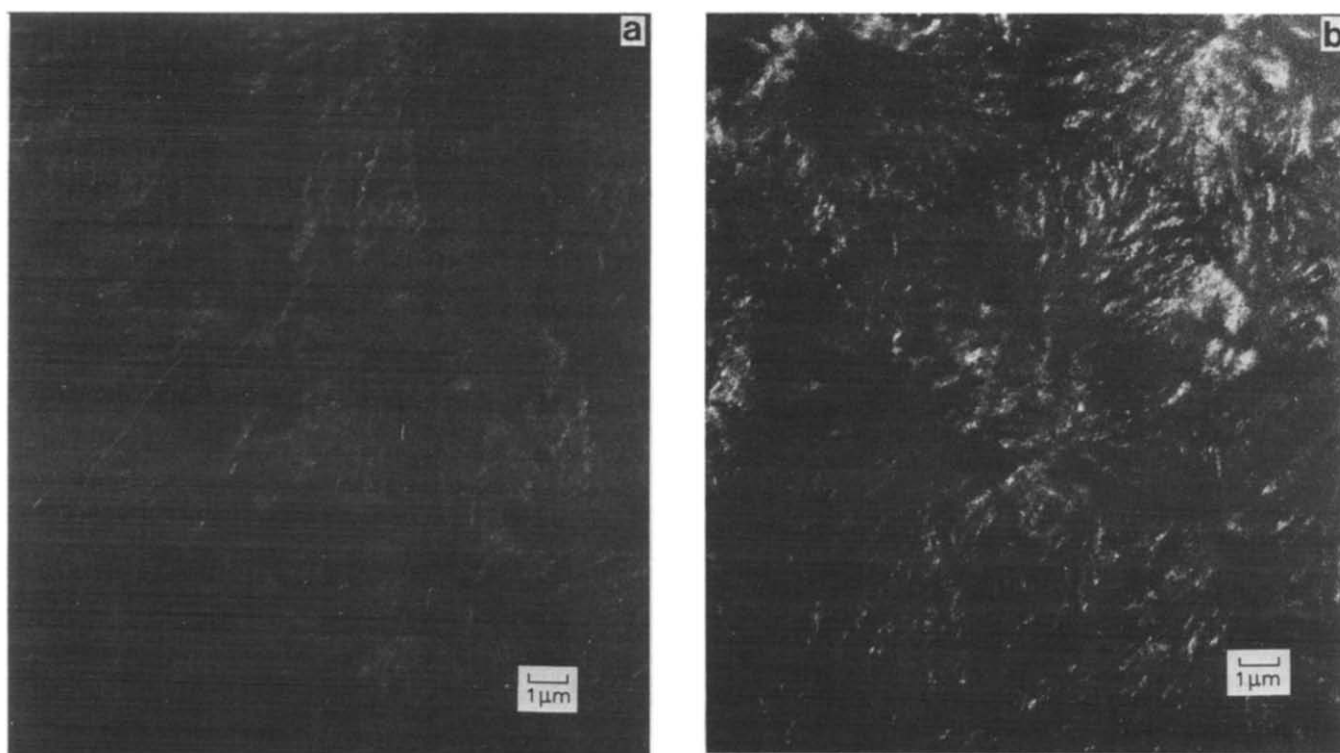
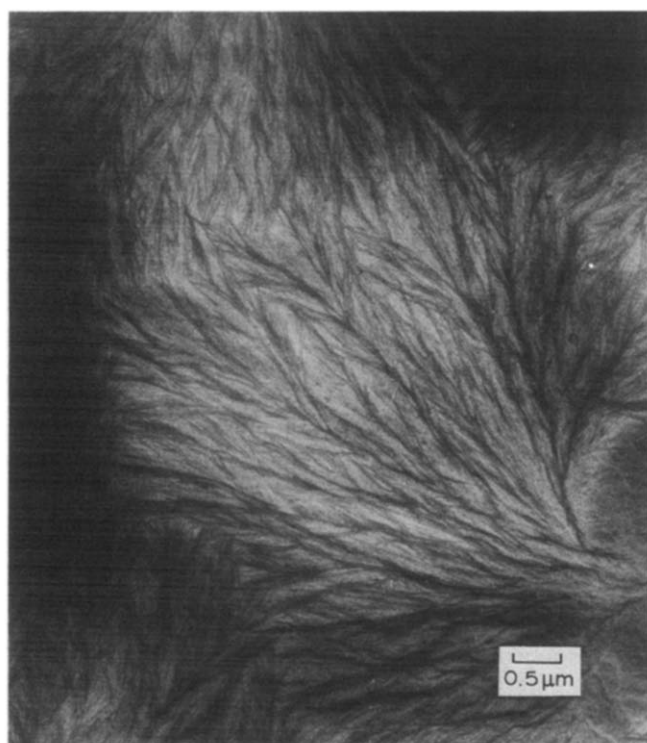


Figure 4 Bright-field electron micrograph of 1,2-dichloroethane solution cast Estane 5712 thin film shadowed with C/Pt after being aged at room temperature for (a) one day and (b) 3 months



**Figure 5** Dark-field diffraction contrast electron micrograph of 1,2-dichloroethane solution-cast Estane 5712 thin films aged at room temperature for (a) one day and (b) 3 months



**Figure 6** Bright-field electron micrograph of Estane 5712 thin film stained with  $\text{OsO}_4$

pendent. In brief, the material is soft and rubbery when fresh and hardens with time. The Young's modulus and yield stress of the compression moulded film are plotted as functions of room-temperature ageing in *Figures 10* and *11* respectively. It is seen that both the modulus and yield stress increase rapidly over a period of about three days

after which they increase at a much lower rate. They reach their limiting values in about one month. The Young's modulus and yield stress of the solution-cast films as functions of ageing time are also shown in *Figures 10* and *11*, respectively, with similar results.

#### *Estane 5707*

Neither the thick nor the thin Estane 5707 films cast from the solution at room temperature contain a crystalline phase as judged from their WAXD and electron diffraction patterns and d.s.c. measurements. These samples remain amorphous even after an extended period of ageing (up to 6 months) at room temperature or annealing (up to 3 days) at elevated temperatures ( $90^\circ\text{C}$  to  $200^\circ\text{C}$ ) in a nitrogen atmosphere. However, the SAXS pattern of the thick films cast from the solution at room temperature shows a scattering intensity maximum corresponding to a Bragg spacing of  $\approx 104 \text{ \AA}$  (*Figure 12*) which is usually interpreted as the average spacing between centres of two neighbouring like domains. The surface of thin films cast from DMF solution in air at room temperature showed no structure. The use of dark field microscopy to observe domains in such films proved futile. The phase contrast imaging techniques suggested by a number of researchers<sup>27,28</sup> also failed to provide any positive result.

Films cast from the solution at  $135^\circ\text{C}$  by slow evaporation contain a crystalline or paracrystalline phase. D.s.c. scans of such films show a broad melting transition at  $150^\circ\text{C}$ – $170^\circ\text{C}$  which is usually attributed to the melting of paracrystalline MDI–BDO hard-segment domains<sup>7,10</sup> (*Figure 13*). There is no evidence of PTMA crystallization. Electron diffraction patterns show the presence of a paracrystalline phase in an amorphous matrix. A typical electron diffraction pattern taken from an area containing paracrystalline hard-segment domains is shown in

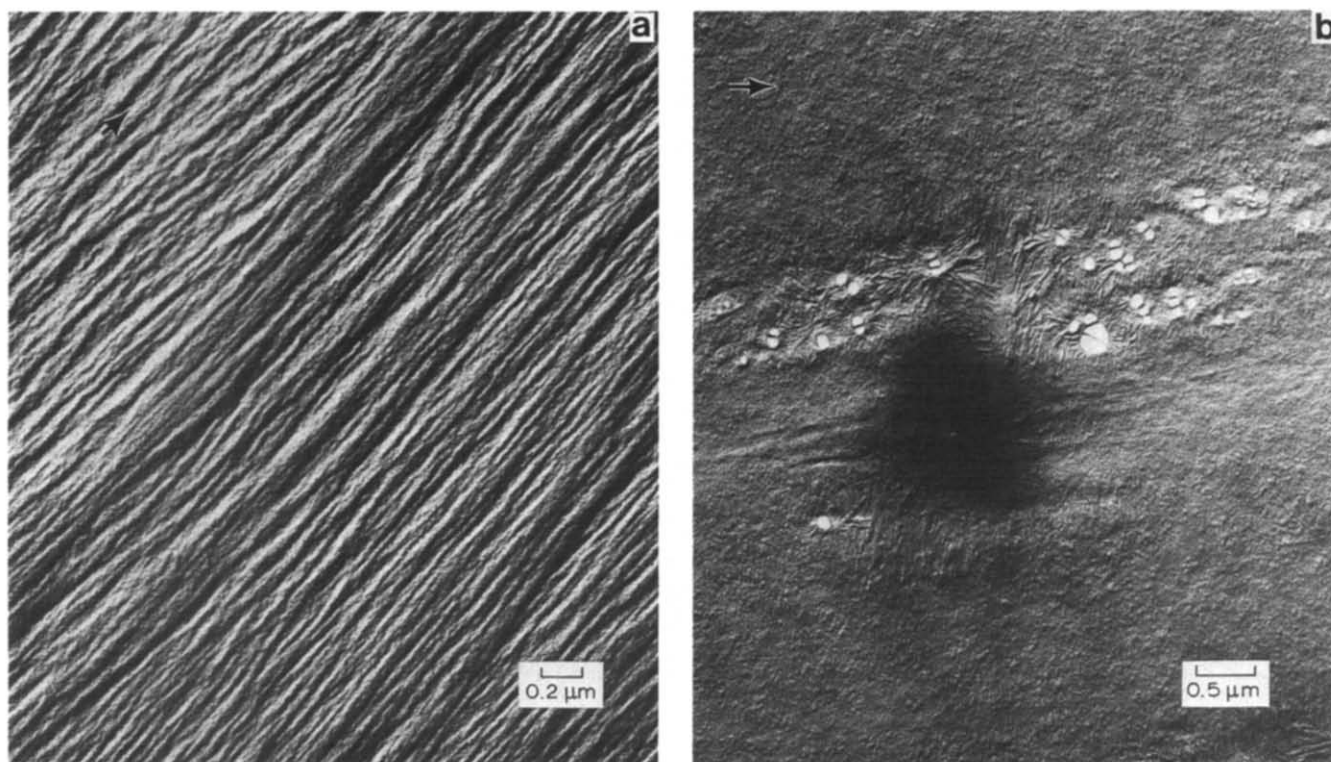


**Figure 7** Bright-field electron micrograph of 1,2-dichloroethane solution-cast Estane 5712 thin film drawn 4 × and then shadowed with C/Pt after being aged at room temperature for (a) one day and (b) 3 months. Arrow denotes draw direction

Figure 14. Only one distinct crystalline diffraction ring corresponding to a Bragg spacing of 4.51 Å can be seen. This indicates that the MDI-BDO hard segments in Estane 5707 form only poorly developed crystalline structures. A typical dark-field diffraction contrast electron micrograph taken with the one crystalline diffracted beam is shown in Figure 15. The bright image is believed to be that of an aggregate of paracrystalline hard segment domains. To achieve reasonable contrast in the dark-field micrographs, within the limits of the beam induced radiation damage, the highest feasible magnification which could be used was 2000 ×.

Unlike the case of Estane 5712, the OsO<sub>4</sub> staining technique fails to stain the amorphous polyester domains in Estane 5707. Thin films of Estane 5707 which have been treated with OsO<sub>4</sub> do not appear to be any different from those which have not been treated.

## DISCUSSION

### Estane 5712

The SAXS period obtained is similar to those obtained by other workers<sup>7,9,15</sup>. The 200 Å value is generally interpreted as the average spacing between centres of neighbouring like domains. The fact that such a SAXS intensity maximum is observed in well aged films but not in freshly cast or freshly heat moulded ones suggests dissolution or high temperature disrupts the original domain structure in the material and that subsequent phase separation and domain formation does not occur instantaneously at room temperature but require a finite period of time. With regard to the time dependence of SAXS in polyurethanes following heat treatment, Wilkes and Emerson<sup>35</sup> present a similar interpretation.

PTMA can crystallize in two crystalline polymorphs

designated as the α and β form by Kim<sup>36</sup>. Minke and Blackwell<sup>34</sup> discovered, in a polyurethane similar to Estane 5712 but with the PTMA segments of  $M_n = 7000$ , that the α polymorph melts at 58°C while the β polymorph melts at 49°C. The β form is the unstable form and tends to transform into the stable α form at room temperature. Our d.s.c. and electron diffraction results indicate that the only crystalline phase present in Estane 5712 is the β form PTMA crystalline domains. No transformation into the α form was detected even after ageing for over a year. The difference between the PTMA segment length and hard-segment content in Estane 5712 and those in the sample studied by Minke and Blackwell is presumably the reason for the stability of the β form PTMA crystals. The d.s.c. scans also reveal an increase in the heat of transition and the peak melting temperature with ageing. This indicates an increase in the size and crystallinity of the soft-segment domains. Considerable molecular motion in the soft-segment domains is thus possible at room temperature. Hydrogen bonding, which would significantly restrict molecular motion, is not likely to occur extensively among the hard segments presumably because they are short. A decrease in the soft-segment  $T_g$  with age in the compression moulded samples implies a higher degree of phase separation is achieved. The fact that the soft-segment  $T_g$  in the solution-cast films does not show any measurable change is believed to be the net result of two factors – the temporary retention of a trace of the solvent (1,2-dichloro-ethane) in the freshly cast films and the effect of phase segregation. The solvent acts as a plasticizer which lowers the  $T_g$  in the freshly cast films. With time, it evaporates completely. Meanwhile, phase separation of soft and hard segments progresses and the soft-segment  $T_g$  stays at about the same value even when the samples become devoid of plasticizer.

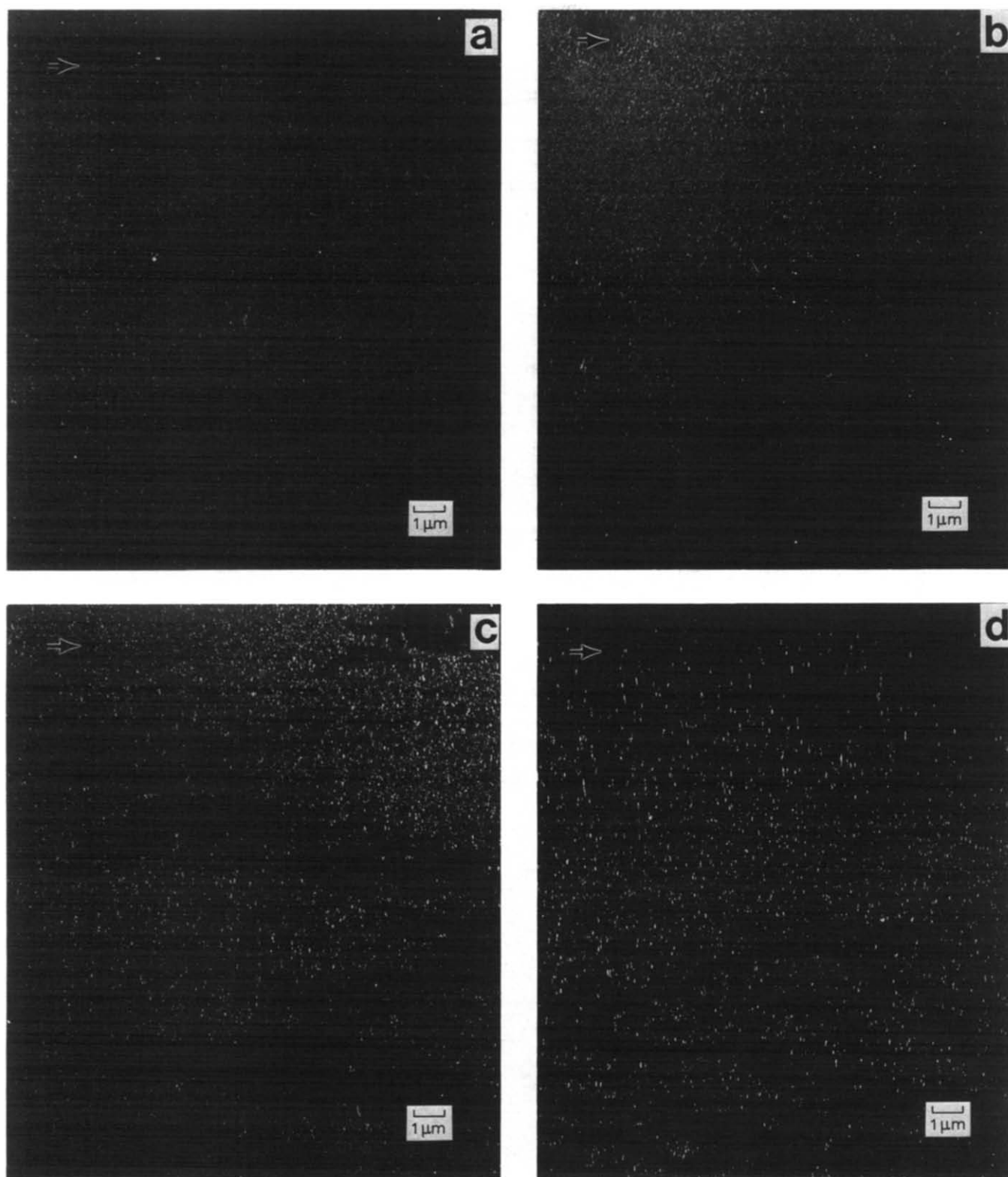


**Figure 8** Dark-field diffraction contrast electron micrograph of 1,2-dichloroethane solution-cast Estane 5712 thin films drawn  $4\times$  and aged at room temperature for (a) one day; (b) 10 days; (c) 30 days and (d) 40 days. Imaging was done with the 3.74 Å (020) and 418 Å (110) equatorial reflections from  $\beta$  PTMA crystals. Arrow denotes draw direction

The domains observed by dark-field microscopy are formed by the aggregation and subsequent crystallization of the PTMA soft segments. Dark-field micrographs of oriented samples (Figure 8a-d) show that the PTMA domains therein are lamellae of thickness up to 300 Å while their width can be as high as 2000 Å. The PTMA segments ( $M_n = 3100$ , calculated average extended chain

length = 227 Å) must be aligned parallel to the thickness direction and there can be no chain folding within the crystalline domains. If chain folding is present in Estane 5712, the folds themselves must involve the hard segments. The observation of PTMA crystals of up to 300 Å in thickness is not an unreasonable result since the PTMA molecular weight has a distribution and soft segments



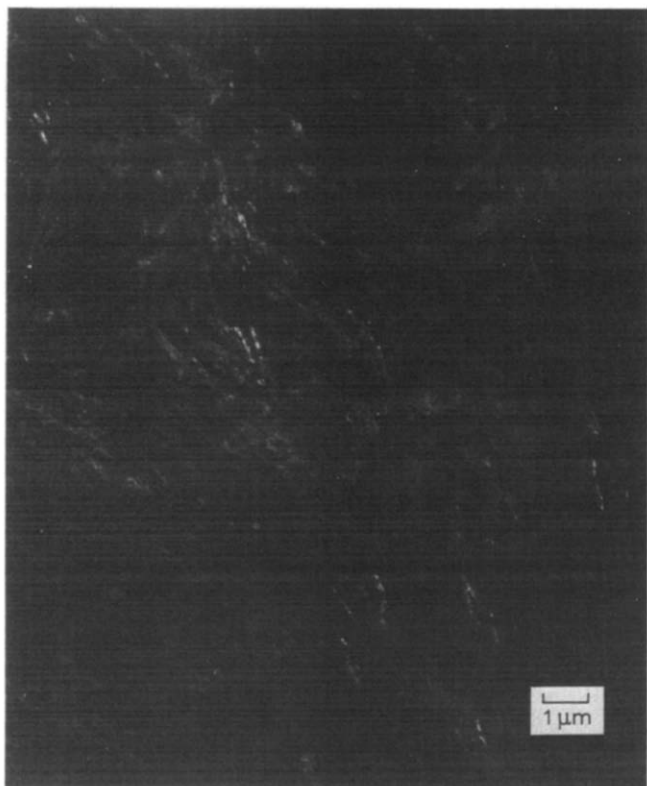


**Figure 9** Typical dark-field diffraction contrast micrograph of a solution cast Estane 5712 thin film drawn 4×, aged for ten days at room temperature and subsequently annealed taut at 90°C for 30 min in a nitrogen atmosphere

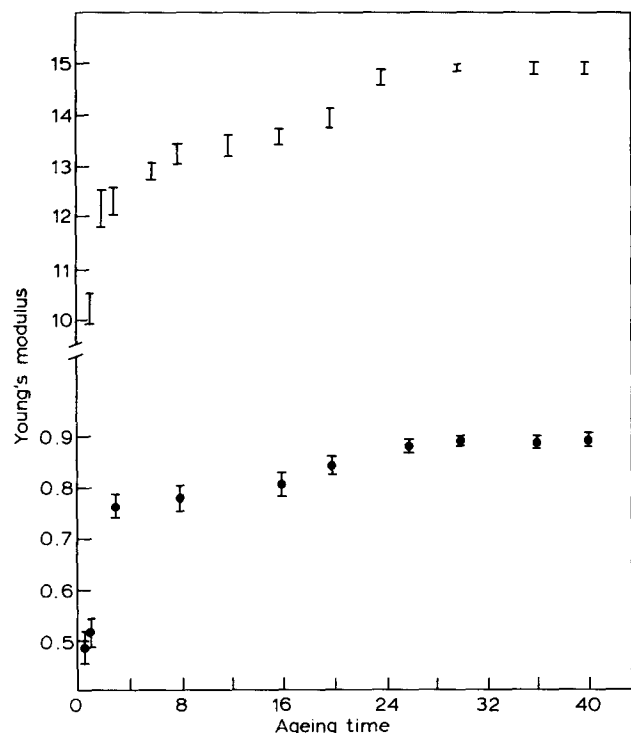


**Figure 10** Variation of Young's modulus (measured in  $10^8 \text{ Nm}^{-2}$ ) of Estane 5712 with ageing time (measured in days)

considerably longer than the average 227 Å may be present. However the results suggest the longer segments seek each other out to form the larger crystals, although this would seem difficult since there should be a distribution in soft segment lengths within any given molecule.

Crystalline MDI-BDO copolymer is believed to melt at above 200°C<sup>6,10</sup>. The absence of such a melting transition in our d.s.c. scans shows that the hard-segment domains in Estane 5712 are not crystalline. The hard segments, with an extended chain length of either 14 Å or 36 Å, are presumably too short to crystallize. The observation that annealing of a drawn sample at 90° completely destroys the previously induced soft-segment orientation implies that the MDI-BDO hard-segment domains are unstable to temperatures at least this low.

Although considerable effort has been devoted by a number of researchers<sup>22-24</sup> to develop staining techniques which may enable the direct observation of domains in typical polyurethanes in the electron microscope, a reliable and acceptable method has yet to be found. The crystalline PTMA domains in Estane 5712 have been successfully stained with OsO<sub>4</sub> here by modifying a technique reported by Wegner *et al.*<sup>33</sup>. The result

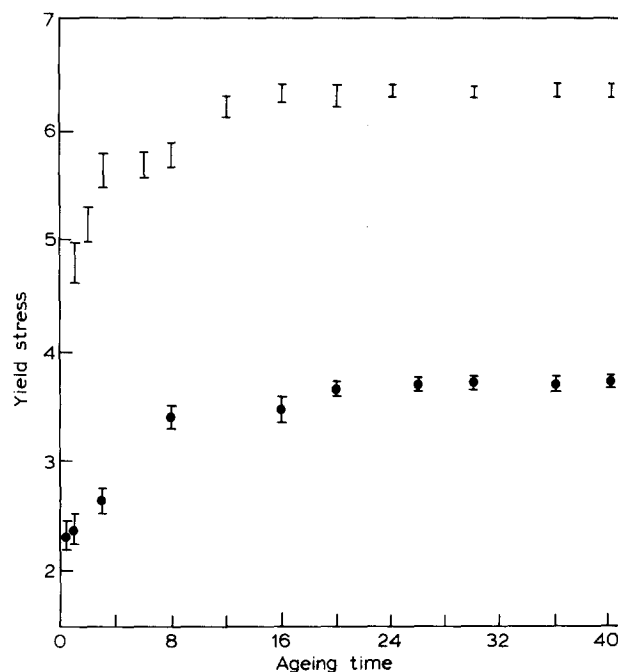


**Figure 11** Variation of the yield stress (measured in  $10^6 \text{ Nm}^{-2}$ ) of 1,2-dichloroethane solution-cast Estane 5712 thick films with ageing time (measured in days)

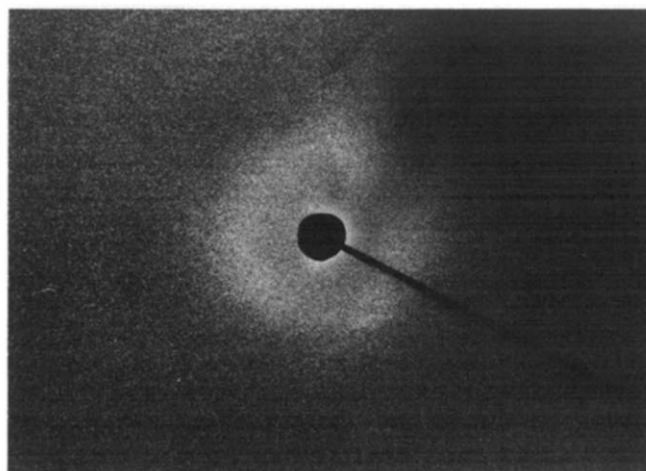


**Figure 12** SAXS pattern of Estane 5707 thick films cast from DMF solution at room temperature

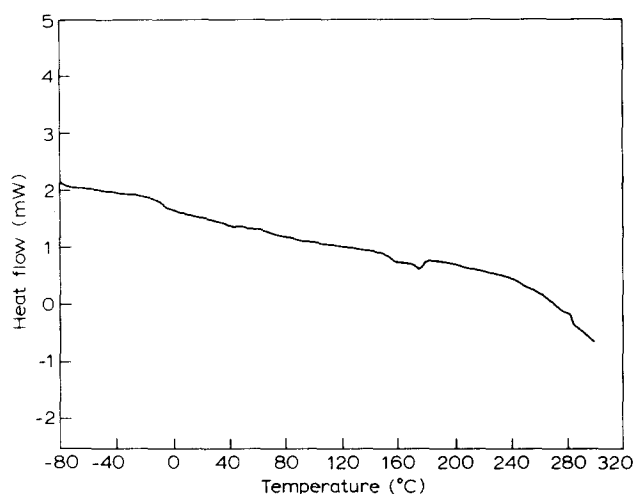


**Figure 13** D.s.c. scan of Estane 5707 film cast from DMF solution at 135°C by slow evaporation

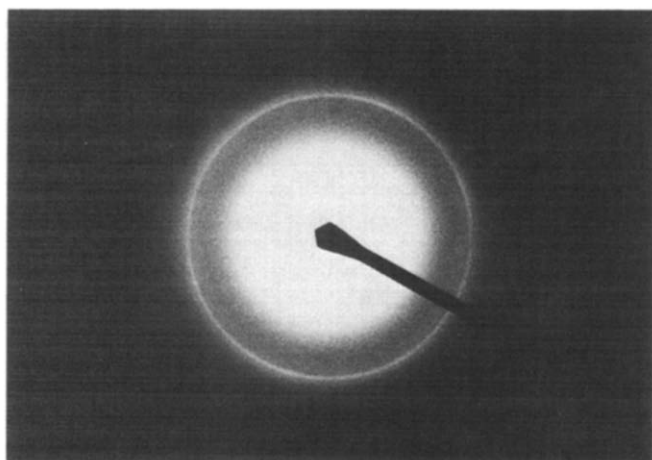


**Figure 14** Electron diffraction pattern of the paracrystalline phase in Estane 5707 thin film cast from DMF solution at 135°C by slow evaporation

(Figure 6) is in excellent agreement with that from dark-field microscopy (Figure 5), the lamellae being stained through their entire thickness. This, however, is surprising since one would not expect the crystalline regions to stain. It is believed this result shows that allyl amine is absorbed by the polyester segments during solution casting and is retained in the polyester phase during crystallization.

The time dependence of the mechanical properties of Estane 5712 further augments the conclusion drawn from SAXS, d.s.c. and TEM studies which show that high temperature or dissolution disrupts the original domain structure in the material and allows intermixing of soft and hard segments. Upon cooling to ambient temperature or evaporation of the solvent, a substantial period of time is required for the two types of segments to separate and reestablish the domain structure which, in turn, is seen to significantly influence the mechanical properties. Both the Young's modulus and yield stress increase monotonically with increasing degree of phase segregation. A well developed domain structure is directly responsible for the high tensile strength of polyurethanes. The Young's modulus of the compression moulded films is higher than that of the solution cast films by a factor of 10. This is

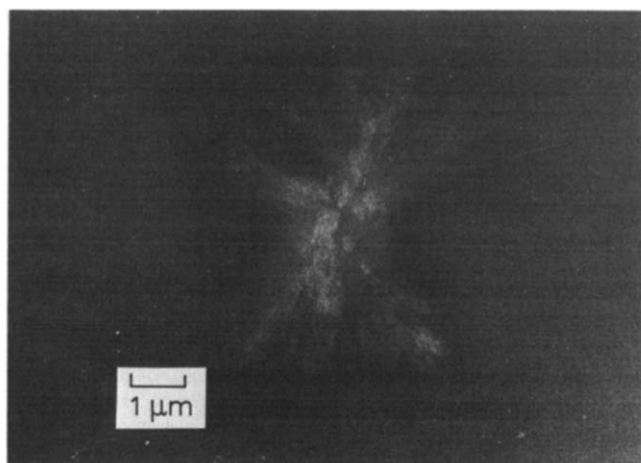


**Figure 15** Dark-field diffraction contrast electron micrograph of Estane 5707 thin film cast from DMF solution at 135°C by slow evaporation showing an aggregate of paracrystalline hard-segment domains

thought to be a result of the retention of a trace of solvent by the latter.

#### Estane 5707

The intensity maximum observed in the SAXS pattern of Estane 5707 suggests that phase separation also occurs in this polymer but that the average spacing between centres of neighbouring like domains is  $\approx 104 \text{ \AA}$ . Since the average extended chain length of the PTMA segments in this sample is  $117 \text{ \AA}$ , while that of the MDI-BDO hard segments is  $58 \text{ \AA}$ , this suggests that the segments may not be fully extended in the polyurethane. Since the content of MDI-BDO hard segments is higher in Estane 5707 than in Estane 5712, these hard segments, capable of hydrogen bonding, can form stable domains which act as tie points, considerably restricting molecular motion. Hence neither ageing nor annealing at high temperatures could greatly alter the morphology and physical properties of the material. Only when the material is dissolved are such hydrogen bonded hard-segment domains disrupted, allowing some molecular rearrangement. Even when Estane 5707 is cast from solution at elevated temperatures in the presence of the vapour of a good solvent (DMF) crystallization of the MDI-BDO hard segments is still sluggish, resulting in only fibrillar aggregation of presumably paracrystalline domains embedded in a largely amorphous matrix.

Since the calculated extended length of the MDI-BDO hard segments is  $58 \text{ \AA}$ , the average thickness of the hard-segment domains would be of a comparable magnitude. Thus individual hard-segment domains may not be directly observed because of their small size and the limited resolving power of the electron microscope at the low magnification used. However, sufficiently large, commonly oriented clusters of such domains can be directly observed with little difficulty (Figure 15).

That the amorphous PTMA domains failed to be stained with the same technique successful for crystalline PTMA domains is not yet well understood and requires further study.

#### ACKNOWLEDGEMENT

Appreciation is expressed to the National Science Foundation (Polymer Program) for financial support of this

research and to the University of Illinois Materials Research Laboratory and Center for Electron Microscopy for use of their facilities.

## REFERENCES

- Schollenberger, C. S., Scott, H. and Moore, G. R. *Rubber World* 1958, ??, 549
- Cooper, S. L. and Tobolsky, A. V. *J. Appl. Polym. Sci.* 1966, **10**, 1837
- Schollenberger, C. S. and Dinbergs, K. *J. Elastoplastics* 1973, **5**, 222
- Schollenberger, C. S. and Dinbergs, K. *J. Elastomers and Plastics* 1979, **11**, 58
- Shimanskii, V. M., Shkil'nik, S. I. and Kozavov, S. B. *Soviet Rubber Technol. (English Transl.)* 1967, **26**, 29
- Clough, S. B. and Schneider, N. S. *J. Macromol. Sci. (Phys.)* 1968, **B2**, 553
- Clough, S. B., Schneider, N. S. and King, A. O. *J. Macromol. Sci. (Phys.)* 1968, **B2**, 553
- Schollenberger, C. S. 'Adv. in Chem. No. 176, Multiphased Polymers' (Eds. S. L. Cooper and G. M. Estes), 83 (1979)
- Bonart, R. *J. Macromol. Sci. (Phys.)* 1968, **B2**, 115
- Bonart, R., Morbitzer, L. and Hentze, G. *J. Macromol. Sci. (Phys.)* 1969, **B3**, 337
- Bonart, R., Morbitzer, L. and Muller, E. H. *J. Macromol. Sci. (Phys.)* 1974, **B9**, 447
- Bonart, R. and Muller, E. H. *J. Macromol. Sci. (Phys.)* 1974, **B10**, 177
- Bonart, R. and Muller, E. H. *J. Macromol. Sci. (Phys.)* 1974, **B10**, 345
- Harrell Jr., L. L. *Macromolecules* 1969, **2**, 607
- Wilkes, C. E. and Yusek, C. S. *J. Macromol. Sci. (Phys.)* 1973, **B7**, 157
- Seymour, R. W., Estes, G. M. and Cooper, S. L. *Macromolecules* 1970, **3**, 579
- Van Bogart, J. W. C., Lilaonitkul, A. and Cooper, S. L. 'Adv. in Chem. No. 176, Multiphased Polymers' (Eds. S. L. Cooper and G. M. Estes), 3, (1979)
- Abouzhar, S. and Wilkes, G. L. 'Segmented Copolymers with Emphasis on Segmented Polyurethanes', to be published
- Schneider, N. S., Desper, C. R., Illinger, J. L., King, A. O. and Barr, D. *J. Macromol. Sci.-Phys.* 1975, **B11**, 527
- Cooper, A. L., Briber, R. M., Thomas, E. L., Zdrahala, R. J. and Critchfield, F. E. *Polymer* 1982, **23**, 1060
- Briber, R. and Thomas, E. L. *J. Macromol. Chem.* 1981, **182**, 231
- Koutsky, J. A., Hien, N. V. and Cooper, S. L. 'Adv. in Chem. No. 176, Multiphased Polymers' (Eds. S. L. Cooper and G. M. Estes), 3, (1979)
- Aggarwal, S. L. *Polymer* 1976, **17**, 938
- Fridman, I. D. and Thomas, E. L. *Polymer* 1980, **21**, 388
- Heindenreich, R. D. 'Fundamentals of Transmission Electron Microscopy', Interscience, New York, p. 140 (1964)
- Erickson, H. P. and A. Klug, A. *Ber. Bunsen. Gesell.* 1970, **74**, 1129
- Miles, M. J. and Petermann, J. *J. Macromol. Sci. (Phys.)* 1979, **B16**, 243
- Chang, A. L. and Thomas, E. L. 'Adv. in Chem. No. 176, Multiphased Polymers' (Eds. S. L. Cooper and G. M. Estes), 31, 1979
- Thomas, E. L. and Roche, E. J. *Polymer* 1979, **20**, 1413
- Roche, E. J. and Thomas, E. L. *Polymer* 1981, **22**, 333
- Morrison, R. T. and Boyd, R. N. 'Organic Chemistry', 2nd edn., Allyn and Bacon, 1966
- Blackwell, J. and Nagarajan, M. R. *Polymer* 1981, **22**, 202
- Wegner, G., Zhu, L.-L., Lieser, G. and Tu, H.-L. *Makromol. Chem.* 1981, **182**, 231
- Minke, R. and Blackwell, J. *J. Macromol. Sci. (Phys.)*, 1979, **B16**, 407
- Wilkes, G. L. and Emerson, J. A. *J. Appl. Phys.* 1976, **47**, 4261